ESTIMATION OF SEAWATER LEVEL ON SEA FARMS USING L-BAND RADAR INTERFEROMETRY

SANG-WAN KIM and JOONG-SUN WON

Department of Earth System Sciences, Yonsei University
134 Shinchon-dong, Seodaemun-gu, Seoul, 120-749, Korea
sangwan@yonsei.ac.kr

Abstract

Satellite radar interferometry data shows a strong coherent signal on oyster sea farms where artificial structures installed on the bottom. We obtained 21 highly coherent interferograms from eleven JERS-1 SAR data sets despite of large orbital baseline (~2 km) or large temporal baseline (~1 year). The phases observed in sea farms are probably induced by double bouncing on sea surface, and consequently reveal a tide height variation. To restore the absolute sea level changes we counted the number of wrapping by exploiting the intensity of backscattering. Backscattering intensity is closely correlated with the change in water surface height, while interferometry gives the detailed variation within the limit of 2π (or 15.3 cm). Comparing the radar measurements with the tide gauge records yielded a correlation coefficient of 0.96 and an rms error of 6.0 cm. The results demostrate that radar interferometry is promising to measure sea level.

Key Words: Sea level change, Interferometry, Sea farm

I. INTRODUCTION

SAR interferometry (InSAR) has been applied successfully to estimate subtle deformation on land induced by earthquakes, volcanic activity, aquifer systems, and etc. (Massonnet et al., 1993; Amelung et al., 1999; Sandwell et al., 2000). On the oceanographic applications, SAR imagery has also helped to detect ocean features such as internal waves, eddies and currents, surface wind stress and oilslicks, while satellite radar altimetry such as TOPEX-POSEIDON has been used to measure the height of the sea surface (Robinson, 1995). Although the radar interferometric measurement on sea surface has not be considered feasible, Alsdorf et al. (2000, 2001a, 2001b) recently demonstrated that interferometric phases of L-HH SAR were correlated with centimeter-scale water height changes in the Amazon flooded riverine.

Along the south coast of the Korean Peninsula, a number of sea farming sites are being operated. The structure of our interest is a oyster sea farm that is composed of horizontal and vertical wood bar of about 10 cm in diameter, staying about 1-2 m above seawater surface and attached on the sea bottom. Oyster farms normally consist of fifty to one hundred bars in array. These structures are not visible by any commercial satellite optical system except high resolution image (~1 m) such as IKONOS. SAR, however, well images the artificial structures under favorable conditions (Figure 1). Especially L-HH SAR system is effective and produces radar interferometric pair. In sea farms, coherent signals, caused by manmade oyster farm

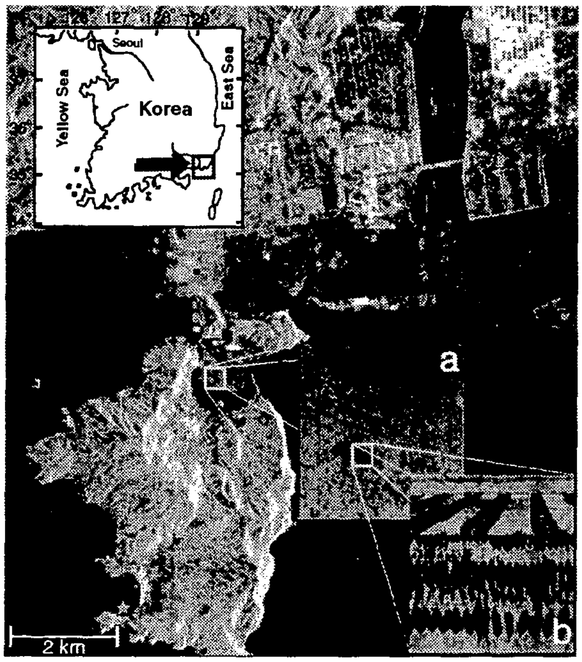

Figure 1. The location map and the JERS-1 multi-image reflectivity map in SAR coordinates. The sea farms and sandbars are marked by red and green dots, respectively. The blue star denotes the tide gauge station. (a) IKONOS image by courtesy of e-HD.com. (b) Field photograph of the oyster farming structures.

structures and comparable to those from land in terms of coherence, were recorded. In this paper, we firstly present the JERS-1 SAR interferometric phase on seawater around Kaduckdo, Korea, and propose a possible application of InSAR to the measurement of instantaneous relative sea level. Validation is provided by in-situ data measured by tide gauge (model: OTT-R20) that is installed near the study area (Figure 1).

II. DATA PROCESSING and ANALYSIS

As shown in Figure 1 the oyster farming structures are imaged as bright scatterers for JERS-1 SAR and the phase is coherent (Figure 2b). The coherent phase values are probably induced by double bounced backscattering after reflecting on the water surface. It is similar to the inundated vegetation introduced by Alsdorf et al. (2000). For the study, we obtained eleven data sets of the JERS-1 SAR between May 2 1996 and July 3 1998. Twenty-one interferometric pairs was successfully generated from them. Table 1 illustrates the time spanning of the interferometric pairs used, their corresponding the altitude of ambiguity (h_a defined by Massonnet et al. (1998)), and the difference of tide height recorded with tide gauge.

Differential Interferograms Generation

Because the seawater level change is regional and the surface is relatively flat, the topographic phase removal is not so critical though two-pass or three-pass DInSAR processing in land surface. Given a reference phase (θ_{ref}) and height (H_{ref}) on a certain ground point and a water surface elevation (H_{water}) of the master scene, the water level change ($\triangle z$) can be estimated through simple arithmetic operation using the following equation:

$$e^{i\theta_d} = e^{i\theta_{ref}} \cdot e^{i\frac{H_{water}-H_{ref}}{h_a}2\pi} \cdot e^{-i\theta_{water}}, \quad (1)$$

$$\triangle z = \frac{\lambda\theta_d}{4\pi\cos(\theta_{inc})}. \quad (2)$$

Where λ is a wavelength of SAR signal , and θ_{inc} is an incidence angle.

During interferogram formation, however, the phase due to the curvature of the earth have to be removed using orbital information. Therefore an accurate baseline is still required but the accuracy of the JERS orbit data are very poor. The orbits were fine tuned by applying a two-pass differential processing to the neighoring land surface so that a flat earth phases and topographic phases are precisely removed. National digital maps at the 1:25,000 scale were used for the two-pass DInSAR. To improve the baseline accuracy, we adopted the method described by Kim et al. (2002). Here we used the tide gauge data for H_{water} of Eq. 1. When using approximation height for H_{water} the low altitude ambiguity generally decreases the error caused by an approximation.

Resulting interferograms contain different phase signatures between seawater and land, and they reveal strong and nearly flat signals. For example, Figure 2a is a differential interferogram of the 9506/9606 pair. Even though topographic phase was eliminated, residual phases on the reclaimed ground caused by subsidence of reclaimed costal land (Kim et al., 2002) and atmospheric artifact were observed. However, as shown in phase profile of Figure 2c a

Table 1. JERS-1 image combinations used for interferometric calculations.

No.	SAR image Master	SAR image Slave	Ambiguity Height (ha)	Time interval (days)	Tide Height Difference (cm)
1	96/05/02	96/06/15	4101.3	44	11
2	96/05/02	97/01/21	151.0	264	11
3	96/05/02	97/06/02	174.9	396	-20
4	96/06/15	96/10/25	258.6	132	-12
5	96/06/15	97/01/21	-148.3	220	0
6	96/06/15	97/06/02	180.6	352	-31
7	96/10/25	97/01/21	-97.6	88	12
8	96/10/25	97/06/02	-215.0	220	-19
9	97/01/21	97/06/02	108.9	132	-31
10	97/06/02	98/05/20	-67.3	352	14
11	97/10/12	97/11/25	-34.8	44	26
12	97/11/25	98/01/08	-79.8	44	-11
13	97/11/25	98/02/21	-264.2	88	16
14	97/11/25	98/07/03	283.4	220	14
15	98/01/08	98/02/21	107.9	44	27
16	98/01/08	98/05/20	-33.8	132	-1
17	98/01/08	98/07/03	72.7	176	25
18	98/02/21	98/05/20	-26.3	88	-28
19	98/02/21	98/07/03	184.5	132	-2
20	98/05/20	98/07/03	21.7	44	26
21	96/05/02	96/10/25	262.1	176	-1

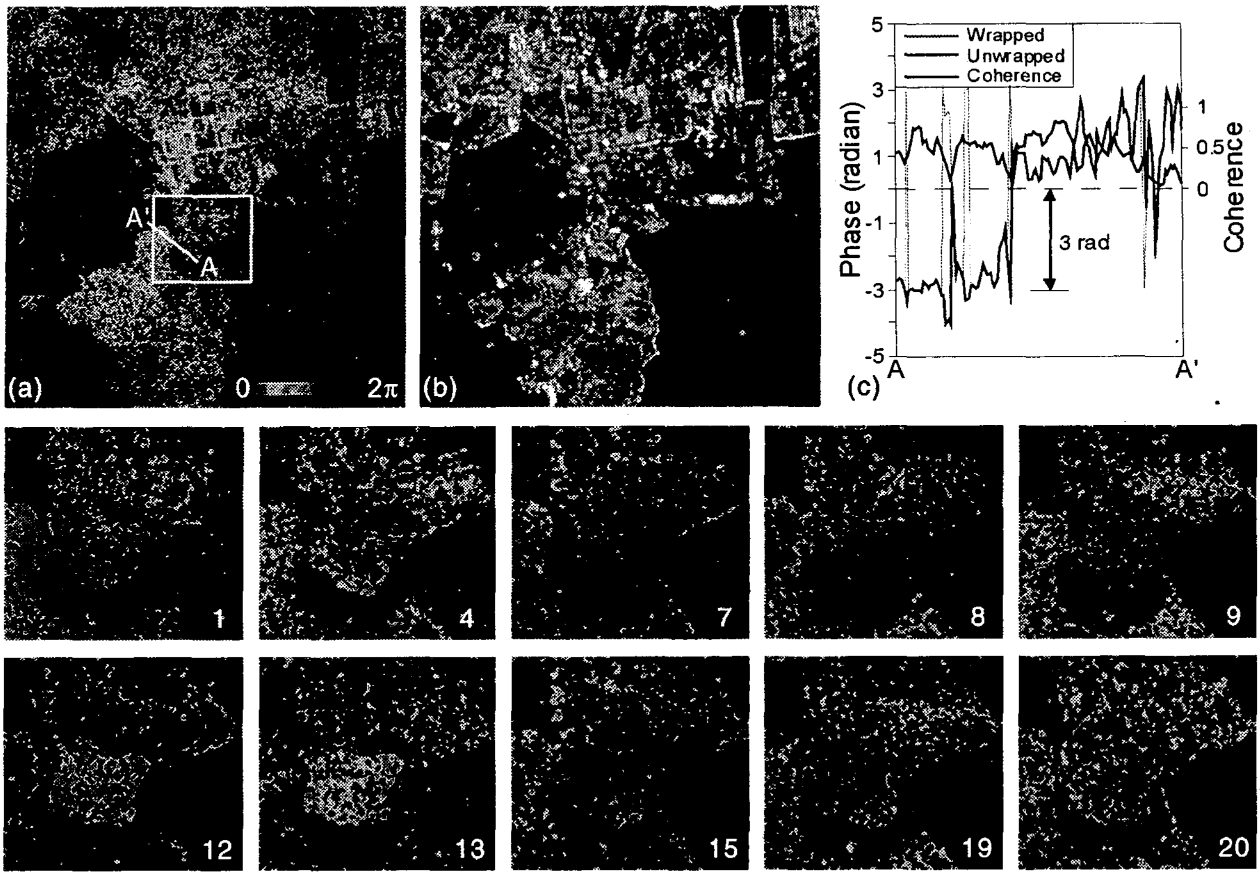

Figure 2. (a) Differential interferogram of the 9605/9606 pair. The box marks the area covered in zoomed image. (b) Average coherence of twenty-one interferometric pair. (c) Profile of phase and coherence values extracted from the line A-A'. Bottom ten images are typical resulting differential interferograms. The number indicated that one in Table 1.

phase difference (~3 radians) indicates a change in seawater level. However the interferometrically measured water level in Figure 2c could have increased by 7.3 cm or decreased by 8 cm because of sign ambiguity. Additional integer multiples of ±15.3 cm are also possible. Among twenty-one pairs used, ten typical interferograms are shown in Figure 2.

Phase Unwrapping

The absolute sea level changes cannot properly be restored by interferometric phases alone because of the discontinuity of phase and the large sea level changes (more than about 15.3 cm corresponding to 2π) in the area of interest. The wrapped differential phases are limited to an estimation of -7.6~7.6 cm changes due to uncertainty of sign (up or down). If water level changes exceed 15.3 cm, then phase unwrapping will be necessary to resolve the inherent 2π ambiguity. TOPEX-POSEIDON altimetry data or consecutive phase within the transition zone (Alsdorf et al., 2001b) can be used for phase unwrapping (Alsdorf et al., 2001a, 2001b).

In our case, the sea water change could be caused by ocean tide that is a time harmonic function distributed with spatially different values, thus altimetry data cannot be used to resolve the ambiguity. Satellite altimetry is usually not very accurate at near coast. In addition because of spatial discontinuity we cannot find the wrapping count between two differential phase group. We have overcome the ambiguity problem to some extent by exploiting radar backscattering (that is, the image brightness). Compared to interferometry, the advantage of the analysis of backscattering is its ability to directly detect the surface height change if the backscattering intensity is proportional to the sea level. The intensity of radar backscattering is usually not a function of single parameter or the length of the exposed bar, because of Bragg scattering in seawater surface. The ambiguity problem, however, can overcome from backscattering intensity with even rough accuracy. Because we cannot obtain accurate sigma naught from JERS-1 SAR (Shimada, 1998), the radar intensity from sea farms was normalized using the statistics of the intensities at seawater and urban land area.

$$R = (I_{seafarm} - I_{seawater}) / (I_{urban} - I_{seawater}). \quad (2)$$

Where I is the peak value of fitted Rayleigh distribution, and their coefficient of determination (Ross, 1987) are all over 0.95. The normalized intensity, *R*, was inversely proportional to the gauged sea level with a correlation coefficient of -0.83 and r.m.s. error of 7.85 cm (Figure 3a). Unfortunately scattering in the study area have exactly not a linear relationship with the tide height since it is affected by oysters growing, the error of tide height (It is not on-site measurement) and Bragg scattering. However, We could thus constrain the number of wrapping counts to one (12 pairs) or two (9 pairs) within 68% confidence interval (Figure 3b). All differential phase within sea farms has been unwrapped by the Flynn's method (Flynn, 1997).

III. RESULTS and DISCUSSIONS

From resulting twenty-one interferograms, the instantaneous sea level changes were estimated for the first time. The comparison of the radar measurements with the tide gauge data that is wrapped ranging from -7.6 cm to 7.6 cm yielded a relatively low correlation coefficient, 0.29 (rms error of 4.2). The possible error sources included the tide gauge measurements, which was not on-site measurements but 5 km away from the test site,

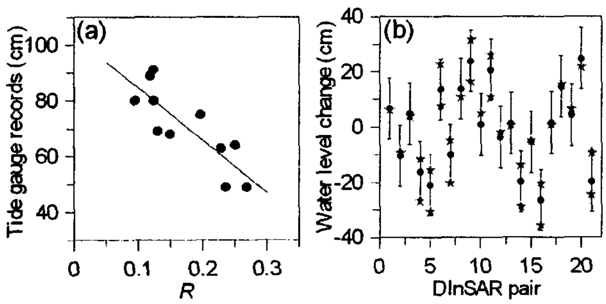

Figure 3. (a) Tide height versus a relatively normalized backscattering (R). (b) The circle and vertical line represents water level change estimated by R values and confidence interval of 68%. The star represents interferometric measurement content with the confidence interval.

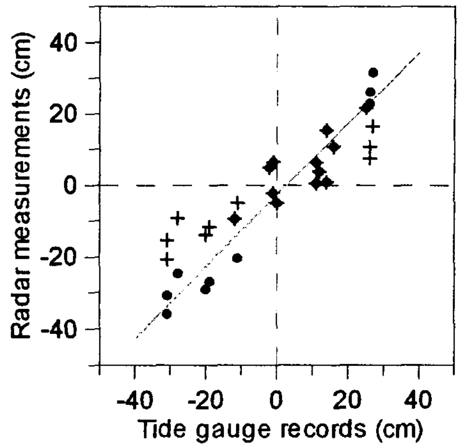

Figure 4. Plot of tide gauge records versus radar measurements. The cross and circle dots represent unwrapped water level changes using one or two wrapping count.

and phase noise error (1.8 cm). The phase error was calculated from the difference between the second order 2-D polynomial modeled planes and radar measurements of high coherence pixels (>0.4) only. Choosing the wrapping count through the proposed method above, the correlation coefficient was improved to be 0.96 with an rms error of 6.0 cm (Figure 4). Here we selected the value favorable to in-situ data when there are two wrapping counts. The results demostrate that the radar interferometry combined with radar backscattering intenstiy is applicable to sea level measurement.

From the result of our research, we can give an answer to some questions raised by Alsdorf (2002): First, can large perpendicular baselines at L-band yield water level changes? Scatterers on the water surface could be considered as pointwise scatterers, thus it would be coherent with unlimited baselines [Ferretti et al., 2001]. Although the critical baseline for JERS-1 L-band SAR system is about 7.5 km (Massonnet et al., 1998), under our research the baseline as long as 2 km offered interferometric phase well. Second, is L-band coherence a function of temporal baseline? Across seasonal growth periods oyster changes will affect coherence besides ocean wind and wave action. Nevertheless we can obtain several interferometric pairs with over one-year temporal baseline. Third, does L-band coherence vary with scatterer density? The coherence in the sea farms averaged 0.32 (maximum: 0.57, minimum: 0.16) estimated in a 5×15 sub-window. Using IKONOS image acquired on February 9, 2001 the array structures of oyster farms were delineate and then the density was obtained. It appear that the coherence is affected by a direction of array as well as scatterer density. JPL AIRSAR data was acquired over the study area with XTI1 mode (L-band and P-band polarimetric mode, C-band TOPSAR mode) on September 30, 2000, as a PACRIM-Ⅱ experiment. The data is being processed by JPL, and is expected to provide clues to backscattering mechanism and the relationship between interferometric phase and tide conditions.

IV. CONCLUSIONS

We observed coherent signals on the seawater from radar measurements. The signal could be considered as double-bouncing returns by the structure of sea farms because the interferometric phase differs from the differential phase observed on land clearly. Considering twenty-one interferograms maintaining high coherence, a temporal and geometrical baseline did not affect the coherence at large. A large baseline (~2 km) can be tolerated in case of a short temporal baseline, conversely a large temporal baseline (~1 year) can be endured in case of a short orbital baseline. A relatively normalized radar backscattering was used to resolve the ambiguity problem of radar interferometry. These observations from JERS-1 SAR provide tide variation of several tens of centimeters in near coast. Comparing the radar measurements with the tide gauge records yielded a correlation coefficient of 0.96 with an r.m.s. error of 6.0 cm. Although a peculiar structure such as sea farms is required, the results show a feasibility of radar interferometry combined with altimetry to sea level measurement on the near coast.

REFERENCES

D.E. Alsdorf, J.M. Melack, T. Dunne, L.A.K. Mertes, L.L. Hess and L.C. Smith, 2000, Interferometric radar measurements of water level changes on the Amazon flood plain, *Nature*, 404: 174-177.

D.E. Alsdorf, C. Birkett, T. Dunne, J. M. Melack and L.L. Hess, 2001b, Water Level Changes in a Large Amazon Lake Measured with Spaceborne Radar Interferometry and Altimetry, *Geophys. Res. Lett.*, 28(14): 2671-2674.

D.E. Alsdorf, L.C. Smith and M. Melack, 2001a, Amazon Floodplain Water Level Changes Measured with Interferometric SIR-C Radar, *IEEE Trans. on Geosci. and Remote Sensing*, 39(2): 423-431.

D.E. Alsdorf, 2002, Interferometric SAR observations of water level changes: Potential targets for future repeat-pass AIRSAR missions *Proceedings for the 2002 AIRSAR Earth Science Applications Workshop*[CD-ROM], JPL Propulsion Laboratory.

F. Amelung, D. L. Galloway, J. W. Bell, H. A. Zebker, and R. J. Laczniak, Sensing the ups and downs of Las Vegas: InSAR reveals structural control of land subsidence and aquifersystem deformation, Geology, 27 (6), 483-486, 1999.

A. Ferretti, C. Prati, and F. Rocca, Permanent Scatterers in SAR Interferometry, IEEE Transactions on Geoscience and Remote Sensing, vol. 39, no. 1, pp. 8-20, 2001

T.J. Flynn, 1997, Two-dimensional phase unwrapping with minimum weighted discontinuity, *J. Opt. Soc. Am. A*, 14(10): 2692-2701..

S.W. Kim, C.W. Lee, J.S. Won, K.D. Min, 2002, Estimation of the Subsidence Rate of Reclaimed Coastal Land using L-band SAR Differential Interferometry, Geophys. Res. Lett., (in review)

Massonnet D. and K.L. Feigl, 1998, Radar interferometry and its application to changes in the earth's surface, Rev. Geophys., 36: 441-500.

Massonnet D., M. Rossi, C. Carmona, F. Adragna, G. Peltzer, K. Fiegl and T. Rabaute, 1993, The displacement field of the Landers earthquake mapped by radar interferometry, Nature, 364: 138-142.

Robinson I.S., 1994, *Satllite oceanography*, John Wiley & Sons Ltd.

Ross S.M., 1987. Introduction to Probability and Statistics for Engineers and Scientists, John Wiley & Sons, Inc., New York

D.T. Sandwell, L. Sichoix, D. Agnew, Y. Bock, and J-B. Minster, 2000, Near real-time radar interferometry of the Mw 7.1 Hector Mine Earthquake, *Geophys. Res. Lett.*, 2(19):3101-3104.

Shimada M., 1998, User's Guide to NASDA's SAR products, Earth Observation research center National Space Development Agency of Japan: 1-24.